Effective of Scribing Wheel Dimensions on the Cutting of AMLCD Glass Substrates

Technical Information Paper

TIP 306
Issued: November 2004
Supercedes: xxxxx

Toshihiko Ono

Corning Japan K.K., Shizuoka Technical Center, 12117, Obuchi, Osuka, Ogasa, Shizuoka, 437-1397, Japan

Kohichi Tanaka

Nagaoka University of Technology, Department of Mechanical Engineering, Materials Science and Engineering Group, 1603-1, Kamitomioka-cho, Nagaoka, Niigata, 940-2188, Japan

Abstract

The scribe and break method for glass cutting is widely used to separate individual Liquid Crystal Display (LCD) panels from a larger mother substrate cell. Optimum glass scribing conditions including scribe wheel dimensions, scribing load, scribing speed, etc, have been determined based on practical manufacturing experience. However, there has been no systematic study to determine the scribing conditions necessary to avoid stray breakage. In this paper, the influence of the scribe wheel angle and diameter upon the scribing and the breaking of an Active Matrix Liquid Crystal Display (AMLCD) glass substrate, Corning Code1737F glass, was experimentally investigated for the case of simple single glass sheet separation. It was determined that an equation including the factors of scribe wheel tip angle and diameter can be used to predict median crack depth as a function of scribe load. It was further found that the breaking force of the scribed sheet was strongly influenced by the residual stress created during scribing. A wheel having a 130° tip angle and 4mm diameter demonstrated the best results for sheet separation in terms of the lowest breaking force without lateral crack propagation. In addition, increasing the time interval between scribing and separating was found to result in an increase in the breaking force required to separate glass substrate.

Introduction

The scribe and break method employing a tungsten carbide wheel is widely used to separate Liquid Crystal Display (LCD) panels from a large mother glass substrate cell. Scribing is a key process to glass separation (cutting). If the scribing conditions are not optimized, clean cutting of the mother cell sometimes becomes difficult due to the formation of lateral

cracks which can propagate and become a source of glass chips. Although scribing conditions such as the scribe wheel dimensions, scribing load, scribing speed etc, have been optimized empirically by manufacturing experience; faulty cutting, in which the cutting line deviates from the scribed line, is still a significant process loss. There have been a few systematic studies to find the influence of scribing conditions on crack creation and propagation. Hara et al in 1950s,[1,2] and Swain et al in 1980s[3,4,5] discussed crack creation and propagation mechanisms during scribing and breaking in the context of contact and fracture mechanics for conventional soda-lime glasses. The results of these studies have not been applied to AMLCD cell separation in which thin glass free from alkali is used.

We have found previously that measuring the breaking force of scribed sheet using a four-point-bending test is an appropriate test for the study of median crack propagation during the breaking process.[6] Furthermore, it has been shown that the experimental breaking force of the scribed sheet was approximately half the breaking force calculated from median crack depth. This was attributed to the effects of residual stress created by wheel indentation.[6,7]

In this study, the influence of scribe wheel dimensions upon median crack creation and propagation was experimentally investigated. This study was designed to find a relation between the scribe wheel variables, the scribe load, and the force for crack creation and propagation. Non-alkaline fusion-drawn glass substrates were used to simulate single sheet separation. We will show in this paper the force required for separation irregularly increased when the residual stress was relaxed by lateral crack propagation. Also, the timing of the lateral crack propagation varied with tip angle of scribe wheel. In contrast to that, the influence of diameter of scribe wheel upon lateral crack propagation was a lesser effect than that of tip angle. In addition, slow growth of lateral cracks was observed after scribing, which caused breaking force increase as the interval time between scribing and breaking processes increased.

2. Experiments

2.1 Sample

1.1 mm thick as-formed Code 1737F glass sheets manufactured by the fusion were used in this study. The density, ρ, and Young's modulus, E, Poisson's ratio, ν, Hardness, H, and Fracture Toughness, K_{IC}, for this glass is listed in Table 1. Here, the reported hardness is the average of the conventional Vickers hardness, H_V, measured at loads ranging from 0.2-9.8N. The substrates for the experiment were in the as-received, or commercially available, condition, i.e. without annealing or other surface treatment.

Table 1
Mechanical properties of Code 1737F and Soda lime glasses.

Glass	Code 1737 F	Soda lime
Composition type	Alkali-earth Aluminoborosilicate	Soda lime silicate
Density, ρ [Mg/m^3]	2.54	2.49
Young's modulus, E [GPa]	72.1	71.5
Poisson's ratio, ν	0.22	0.21
Vickers Hardness, H_V [GPa]	5.5	5.6
Fracture toughness, K_{IC} [MPa m$^{1/2}$]	0.83	0.75

2.2 Preparation of scribed specimens

Single edge notched beam (SENB) type sample pieces 40mm x 50mm in size were obtained from the mother glass sheet by a conventional scribing method. Mother glass sheet size was typically 320x400 mm or 360x465 mm by 1.1mm. A lattice pattern, 40mm x 50mm in pitch was scribed on the mother sheet glass. A median crack line for the four-point-bending-test was formed at the center of the 50 mm-edge on the glass face opposing the lattice pattern. The opposite face was chosen to prevent the growth of the median crack during the separation of the SENB samples from the mother sheet. A scribing speed of 300mm/s and a range of scribing loads from 5N to 25N were used. A Numerically Controlled (NC) scriber, TEC-II, made by Shirai Iron Ind. Co. with tungsten-carbide wheels of the types listed in Table 2 was used to scribe the sample pieces.

2.3 Four point bending test

A load tester, 1310F, made by AIKO Engineering Co., Ltd. was used for the 4-point-bending-test. Dimensions of the upper and lower rods of the load tester were as specified in JIS R 1601 or ASTM C158-80. The specimen was placed on the lower rods with the median crack surface face down, and with the median crack aligned parallel to, and at the center of, the lower rods. This is schematically illustrated in Fig. 1. For every sample, the four-point-bending-test was done within 30 minutes after the introduction of median crack line. This was to prevent slow growth of the median crack by environmental humidity.[8] The specimens were loaded at 5mm/min of cross head speed (minimum loading speed of the tester). The stress intensity factor, K, for the four-point-bending test was evaluated using formula:[9]

$$K = \frac{3P\lambda}{tW^2}\sqrt{\pi c}\cdot F_{IM}(\alpha) \qquad (1),$$

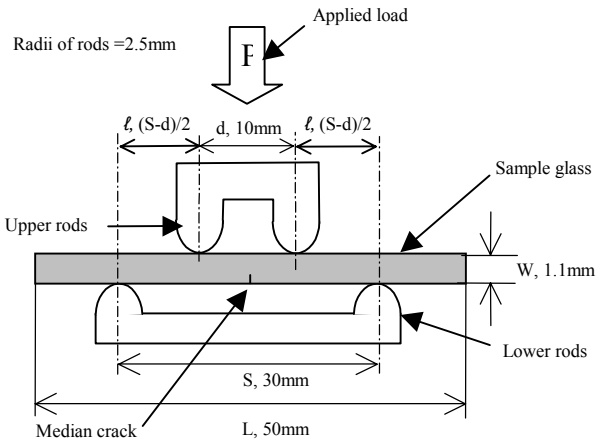

Fig. 1 Schematic illustration of upper and lower rods of four-point-bending test machine.

where P is the applied load, c is the experimentally obtained median crack depth of the cleaved samples, t is sample length (40 mm), W is sample thickness (1.1mm), λ is separation of adjacent upper and lower rods, and F_{IM} (α) is given by Eq. (2).[9]

$$F_{IM}(\alpha) = 1.122 - 1.121\alpha + 3.740\alpha^2 + 3.873\alpha^3 - 19.05\alpha^4 + 22.55\alpha^5 \quad (2),$$

with $\alpha = c/W$.

After recording the breaking force, the fracture surfaces of the broken specimens were observed with a scanning laser microscope (SLM), and the median crack depth was measured at the origination point of the crack propagation. Wallner lines on the fracture surface were used to identify this point.

3. Results and Discussions

3.1 Median crack depth as a function of wheel type

Figure 2 plots the median crack depth, c, as a function of scribe load, P, created by the wheels listed in Table 2. The median crack depth increases with increasing scribe load. It also confirms the common practical knowledge that wheels with smaller diameters and steeper tip angles create deeper median cracks.

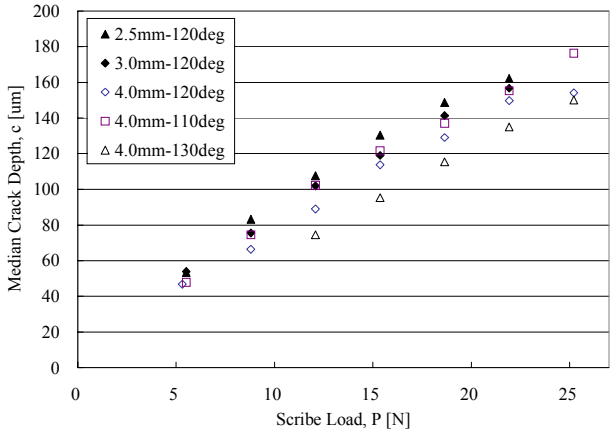

Fig. 2 Median crack depth versus scribe load created by scribe wheels having various tip angles and diameters as listed in Table 2.

Table 2 Angle and diameter of scribe wheels. By Mitsuboshi Diamond Ind. Co, A140 grade

	Tip angle, 2ψ [degree]	Diameter, $2R$ [mm]
Wheel 1	110	4.0
Wheel 2	120	4.0
Wheel 3	130	4.0
Wheel 4	120	2.5
Wheel 5	120	3.0

Although the relationship between median crack depth, scribe wheel dimensions, and scribe load (scribability) has been quantitatively determined for soda-lime glass sheet by Swain,[4] no equivalent study exists for the non-alkaline glass substrates used in AMLCD's. In addition, previous work has not been extended to quantify the degree of difficulty associated with crack propagation (breakability). Finding the relationship between crack creation, crack propagation, and scribing conditions is important for quantitative control of the scribe/break process in LCD cell cutting. Figure 3 shows a typical side view of cleanly cut glass obtained by scribing and breaking. The median crack depth is constant under the plastic core zone, and the Wallner lines (a signature of the scribing process) exhibit a uniform curvature without irregular cracks at the boundary of the plastic core zone. This illustrates the assertion that the median crack can be considered as an edge crack constructed by the connection of half-penny cracks.

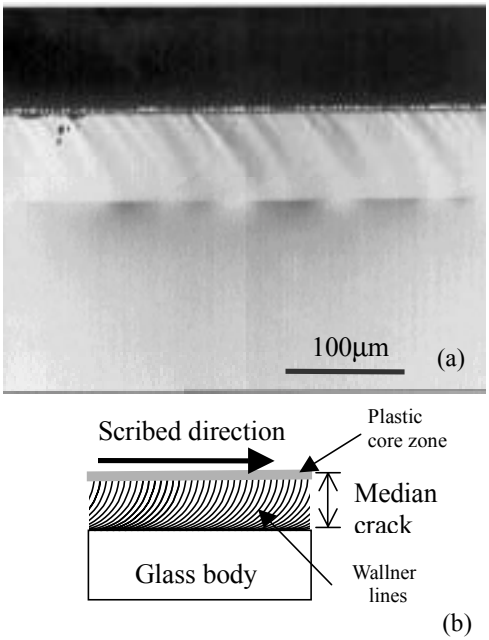

Fig. 3 Fracture surface of the median crack (a), Scanning Laser Microscopic image, (b) schematic illustration of median crack formation by continuously formed half-penny cracks.

3.2 Fracture Mechanics of median crack formation

An approach to indentation fracture toughness proposed by Tanaka[10,11] has been modified to analyze the median crack formed by scribing. Figure 4 schematically illustrates the model. The basic hypothesis is that the stress induced by a scribe wheel having a tip angle, 2ψ,

and a penetration depth, h, is accommodated by plastic

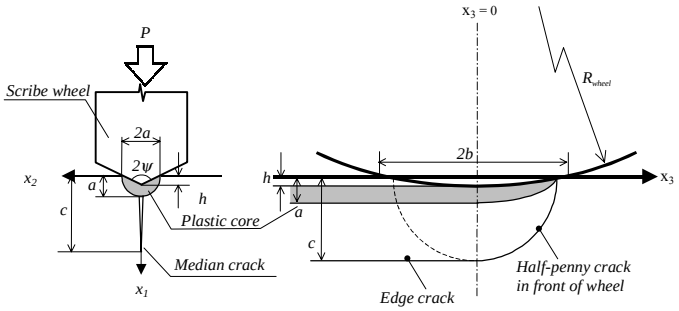

Fig.4 Schematic illustration of scribing process. The plastic zone is exaggerated in this illustration. The depth a is much smaller than both the wheel contact length b, and the crack size c.

straining in the glass (plastic core). The compressed plastic core having radius a, in turn, generates an internal (residual) stress, σ_{22}, by expansion, which is obtained by applying Eshelby's 'inclusion' theory.[12] This residual stress created by the plastic core is the driving force behind the opening of the median crack The median crack to the left side of the wheel axis ($x_3<0$) is an edge crack subjected to concentrated force F along its mouth, corresponding to the plastic core; while that on the right side ($x_3>0$) is considered a half-penny shaped crack. Reversing the sign of the internal stress σ_{22}, inside the plastic core from + to –,[13] we have:

$$F = -(a-h)\sigma_{22} = -a(1-\cot\psi)\sigma_{22} \quad (3),$$

where we take into account the net area of the plastic core acting upon the crack opening. The stress intensity factor for an edge crack is given by:

$$K = 2F/\sqrt{\pi c} \quad (4),$$

and for a half-penny shaped crack is given by:

$$K = (\sqrt{2}-1)F/\sqrt{\pi c} \quad (5),$$

The stress intensity factor of the median crack at the wake of the edge crack just underneath the wheel axis ($x_1=c$, $x_2=x_3=0$) may be evaluated by the arithmetic mean of Eqs. (4) and (5), i.e.:

$$K = \frac{\left(\sqrt{2}+1\right)}{2}\frac{F}{\sqrt{\pi c}} \quad (6),$$

The stress intensity factor at a position far distant from the wheel is the value appropriates for an edge crack expressed by Eq. (4). Thus, the stress intensity factor of the median crack is presumably bound by the two values, Eqs. (4) and (6). From the residual stress σ_{22}, and stress intensity factor, K by Eqs. (4) and (6), two equations were derived. The crack depth using the stress intensity factor for an edge crack is given by:

$$C_U = 4f(\psi)\left[\frac{EP^2}{(1-\nu^2){K_{IC}}^3 R}\right]^{\frac{2}{3}} \quad (7a),$$

and the crack depth using the stress intensity factor for an average of edge and half-penny cracks is given by:

$$C_L = \left(\frac{\sqrt{2}+1}{2}\right)^2 f(\psi)\left[\frac{EP^2}{(1-\nu^2){K_{IC}}^3 R}\right]^{\frac{2}{3}} \quad (7b),$$

where $f(\psi)$ is tip angle factor for the scribe wheel as given by:

$$f(\psi) = \left(\frac{3}{8\sqrt{2}}\right)^{\frac{4}{3}}\left(\frac{1}{\pi}\right)^{\frac{5}{3}}\left[\frac{(1-\cot\psi)^2\cot^2\psi}{(1+\cot\psi)^{\frac{2}{3}}}\right] \quad (8),$$

In addition, a consideration needs to be given for truncation or rounding of the scribe wheel tip angle. The actual wheel tip does not have the ideal shape as indicated by ψ. The truncation or rounding of wheel tip is schematically illustrated in Fig. 5. For this work, we've

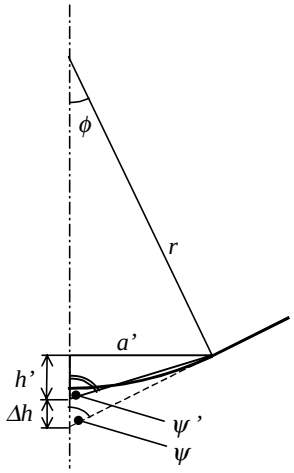

Fig.5 Schematic illustration of truncated tip angle shape. Truncated tip has angle ψ', which is tip angle of a triangle having the same cross sectional area as a rounded tip

assumed that the truncated tip has an angle ψ',

corresponding to the angle of a triangular section having the same cross sectional area as a rounded tip with radius r. The half angle of the effective tip including this truncation factor, ψ', is given by:

$$\cot\psi' = \frac{\pi - 2\psi}{2\cos^2\psi} - \tan\psi \qquad (9),$$

3.3 Influence of wheel tip angle and wheel diameter on scribability

An experiment was designed to investigate the influence of scribe wheel tip angle on median crack depth. The 4mm diameter wheels described in Table 2 were used for this experiment. These results are plotted in Figs. 6 to 8.

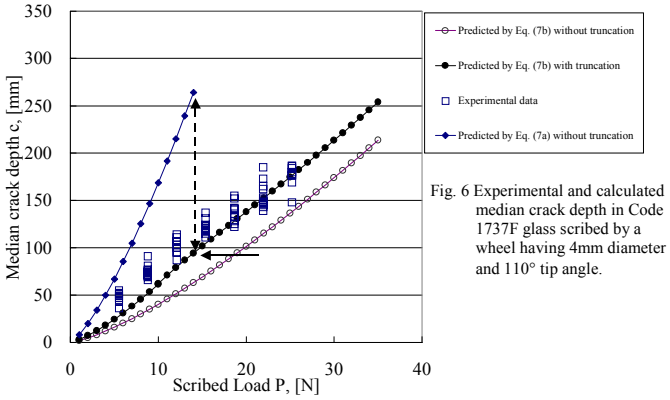

Fig. 6 Experimental and calculated median crack depth in Code 1737F glass scribed by a wheel having 4mm diameter and 110° tip angle.

Also shown on these graphs are the crack depths calculated from Eqs. (7a) and (7b) with $K=K_{IC}$. Values calculated from Eq. (7b) show better agreement with the experimental crack depth values than those calculated from Eq. (7a), even though the actual median crack is an

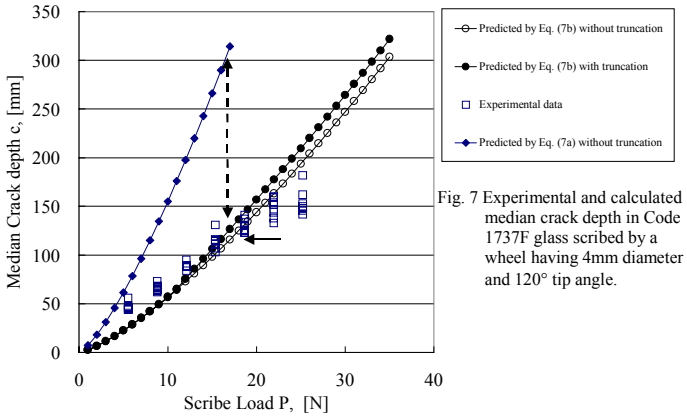

Fig. 7 Experimental and calculated median crack depth in Code 1737F glass scribed by a wheel having 4mm diameter and 120° tip angle.

edge crack, as shown in Fig. 3. Since Eq. (7a) is not the best fit, this leads us to conclude that the stress created by scribing is not completely utilized for median crack formation. The stress used for median crack formation is approximately 40% of the total stress induced by scribing. Approximately 60% of this stress could remain as residual stress around the median crack. Thus, the stress that remains after the creation of the median crack is given by the stress intensity factor K_R:

$$K_R = 0.6K_{IC} \qquad (10),$$

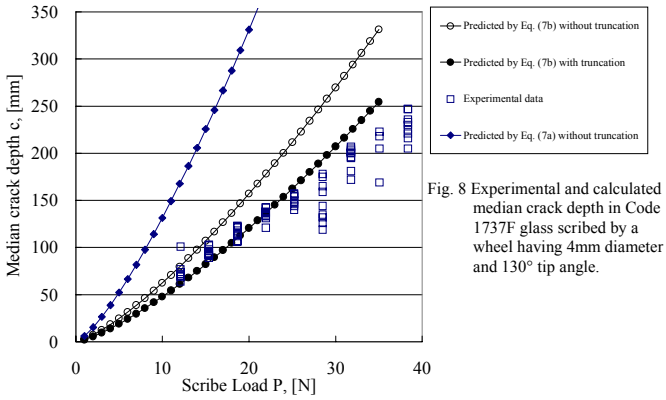

Fig. 8 Experimental and calculated median crack depth in Code 1737F glass scribed by a wheel having 4mm diameter and 130° tip angle.

The median crack depth values as calculated by Eq (7b) including a consideration for the truncation of the scribe wheel tip angle, as explained by Eq. (9) and Δh=2μm, shows even better agreement (solid circles) with the experimental data. This means that the truncation factor should be included to account for the influence of tip angle.

The influence of the tip angle as shown in Eq. (8) with the factor $\cot^2\psi'\cdot(1-\cot\psi')^2/(1+\cot\psi')^{2/3}$, differs from previous analyses in which the tip angle was given by $\cot\psi$ [1] or $\cot\psi^{5/3}$.[4] It is noted that this angle factor becomes zero when the tip angle, 2ψ, is 90°, because h becomes equal to a. Therefore, the Eqs. (8) and (9) are effective only in the range of tip angles commonly used for scribing AMLCD glass substrates (such as 110°-130°). It is also noted that the truncation factor expressed by Eq. (9) is not dependent upon wheel tip wear, because the truncated tip angle, ψ', is constant even as the truncation value, Δh, is increased.

With parameters of scribe load, wheel diameter, tip angle, and glass mechanical properties, the combination of Eqs. (7b) and (9) predict the median crack depth on the same order and range as the experimentally measured values, even with the limitations of tip angle range. By incorporating the appropriate material properties, these equations are applicable to predict the median crack depth in substrates of different glass types. The influence of each material parameter, Young's modulus and stress intensity factor, in the Eqs (7a) and (7b) are analogous with the equation derived by Swain who considered elastic deformation.[14]

Soda-lime glass was selected to confirm the applicability of the present equations for predicting the median crack depth in a substrate of different glass type. The glass was scribed with a 4mm diameter, 110° tip angle wheel. The mechanical properties of the soda lime glass used in the experiment are listed in Table 1.[15] The measured median crack depth as a function of scribe load is plotted in Fig. 9 along with the calculated values. Once again, the median crack depth calculated from Eqs. (7b) and (9) show good agreement with experimental results. This agreement confirms that these equations are applicable to predict the

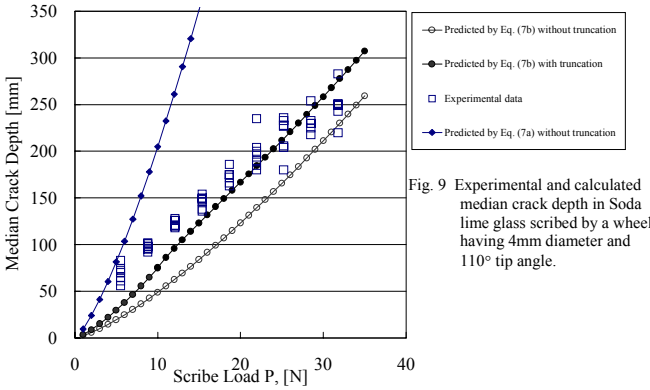

Fig. 9 Experimental and calculated median crack depth in Soda lime glass scribed by a wheel having 4mm diameter and 110° tip angle.

median crack depth in a variety of glasses.

3.4 Influence of wheel angle on breakability

The experimental breaking force required to separate the scribed samples are plotted as a function of the median crack depth in Fig. 10. This figure includes data from samples scribed with wheels having different tip angles. In addition, this figure also includes the breaking force calculated using Eq. (1), *Pc* (dotted line). For samples scribed by wheels having 110° and 120° tip angles, the breaking force dependency on median crack depth follows the lower curve ($0.47P_C$) for samples with median crack depths less than 90mm and 120mm, respectively. For samples with deeper median crack depths, a greater breaking force is required, and the dependency on median crack depth follows the upper curve ($0.8P_C$). Lateral crack propagation was observed to occur in these samples with the deeper median cracks. This crossover (from lower to upper curves) point is indicated with an arrow mark in Figs. 6 and 7. It is proposed that in the region below the arrow mark, the residual stress remains as indicated with the dotted line. In the region above the arrow mark, the residual stress is relaxed by lateral crack propagation, and the breaking force increases. On the other hand, the breaking force of samples scribed by a wheel having a 130° tip angle follows the lower curve for all samples (median crack depths of up to 250μm). Lateral cracks did not propagate for these samples. As a result, in Fig. 8, there is no such boundary.

As mentioned, the cause of the crossover in breaking force dependency for glass scribed by 110° and 120° tip-angled wheels has been explained qualitatively by residual stress relaxation due to lateral crack propagation.[6] At the onset of crack propagation, the critical stress equals the stress induced by bending and the residual stresses present:

$$K_{IC} = K_B + K_R \qquad (11),$$

where K_R is the stress intensity factor due to residual stresses. Since stress intensity factor is linearly proportional to the bending force, K_R becomes βK_{IC} with β=0.17 for the upper curve in Fig. 10 and β=0.53 for the lower curve. As explained in section 3.2, approximately 60% of stress induced during the scribing operation remains around the median crack, and 40% contributes to the median crack creation. This suggests that the residual stress has not been relaxed in the lower curve region, since K_R =0.53K_{IC} is almost equivalent to the residual stress remaining after median crack creation, K_R=0.6K_{IC}. On the other hand, the stress in samples following the upper curve has been somewhat relaxed by lateral crack propagation. However, even in these samples, some residual stress remained as indicated by the difference between this upper curve and the theoretical breaking strength (*Pc*). The experimental breaking force of the scribed glass sheet is strongly influenced by the residual stress induced during scribing.

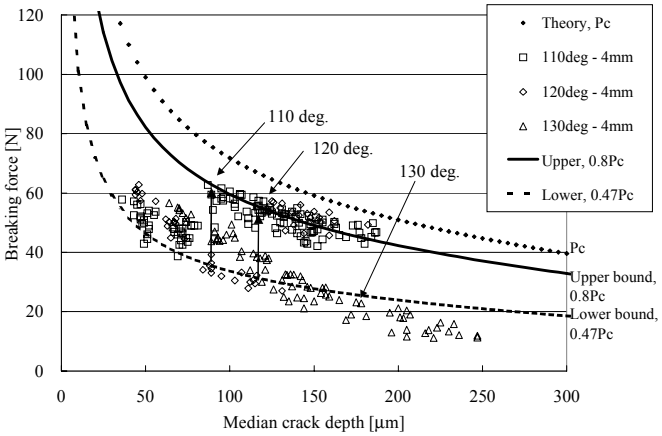

Fig. 10 Breaking force versus median crack depth of the specimens scribed by a wheel having various tip angle; 110° (○), 120° (□), and 130° (△).

3.5 Influence of the wheel diameter to the breakability

As a result, a scribing wheel with 130° tip angle showed the best cuttability for Code 1737F glass substrate. That is, the lowest breaking force was achieved without the formation of lateral cracks. This sample breaking force versus the median crack depth is plotted in Fig 11, for scribing wheels having different diameters. Dependence of breaking force upon the median crack depth is the same as discussed above; the breaking force decreased with increasing median crack depth until the point of lateral crack propagation. Lateral crack propagation tended to be accelerated with smaller wheels, but the effect is much smaller than that of tip angle. Swain confirmed that the mean of indentation pressures for scribe wheels having various tip angles and diameters is independent of load, but varied with tip angle.[3] Swain's results suggest that the creation of the residual stress is strongly related to the tip angle. Therefore, the onset of the breaking force increase due to lateral crack propagation is influenced more by tip angle than by wheel diameter.

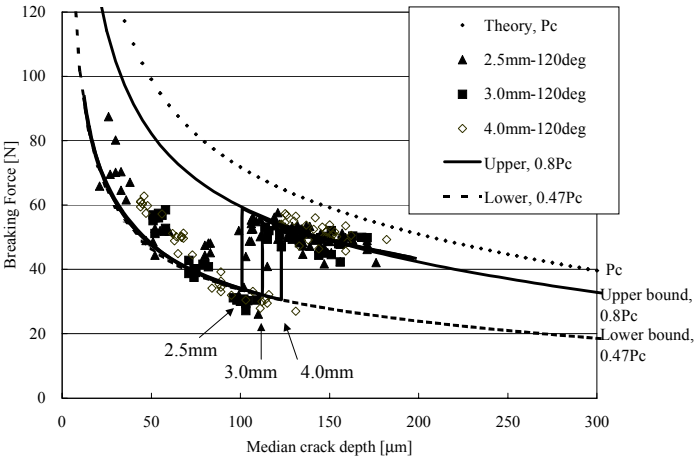

Fig. 11 Breaking force versus median crack depth of the specimens scribed by a wheel having various diameter 2.5mm (▲), 3.0mm (■), and 4.0mm (◇). Tip angle was fixed to 120°.

3.6 Influence of interval time between scribing and breaking

The standard interval of time between scribing and breaking was less than 30 minutes in this study. Fig. 12 is a plot of the breaking force versus median crack depth for samples broken approximately 60 and 90 minutes after scribing with a 2.5mm diameter scribe wheel. The onset point of increasing breaking force was shifted to smaller median crack depth with increasing interval time. It was observed that this phenomenon was due to slow crack growth of lateral cracks after scribing. This mechanism had also been explained by Swain.[5] The phenomena has been explained in manufacturing as the "re-fusion of the median crack", or difficulty of separation of scribed sheet after a longer time interval. It is strongly dependent on the environment, especially humidity.[5, 8] Figure 12 shows that breaking should be done as quickly as possible after scribing, to minimize lateral crack propagation.

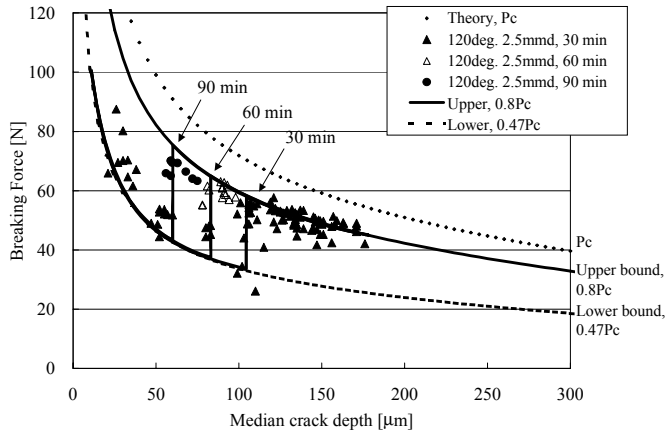

Fig.12 Breaking force versus median crack depth measured 30min(▲), 60 min (•), and 90 min (•) after the scribing. Scribe wheel was 120° tip angle and 2.5mm in diameter.

4. Summary

(1) It was found that the median crack depth by scribing LCD glass substrates could be predicted as a function of scribe load for wheel tip angles between 110° and 130°. This is done by taking into account wheel tip angle (using an equation for considering wheel tip truncation), wheel diameter, and the mechanical properties of the glass substrate.

(2) This equation indicates that the median crack depth is inversely proportional to the 2/3 power of wheel radius and proportional to the tip angle by the factor $\cot^2\psi'\cdot(1-\cot\psi')^2/(1+\cot\psi')^{2/3}$, where ψ' is one half of tip angle including truncation factor given by $\cot\psi' = (\pi - 2\psi)/(2\cos^2\psi) - \tan\psi$.

(3) 40% of the stress induced during scribing is used for median crack creation and 60% remains as residual stress.

(4) The residual stress remaining after median crack creation strongly aids the ease breaking. However, this breaking assist is lost when lateral crack propagation relaxes this stress.

(5) The best cuttability (lowest breaking force) of scribed Code 1737F LCD glass substrate was performed by a wheel having 130 degree tip angle and 4mm in diameter which did not create lateral cracks.

(6) Slow growth of lateral cracks was observed after scribing. Shorter interval between scribing and breaking is effective to decrease breaking force.

Acknowledgement

Author would thank to Drs. Y. Imamura and R. Allaire and P. L. Bocko, and Mr. G. A. Luers of Corning Inc. for their technical comments on the manuscript.

References

1 M. Hara and J. Nakayama, “Study on the Cutting of Sheet Glass (part 1)”, Asahi Glass Co., Research Lab. Report, 6, [1], pp1-11, (1956).

2 M. Hara and J. Nakayama, “Study on the Cutting of Sheet Glass (part 2)”, Asahi Glass Co., Research Lab. Report, 6 [2], pp35-44, (1956).

3 M. V. Swain, “The Deformation Associated with the Scoring of Soda-Lime Float Glass with a Disc Cutter”, Glass Technology, Vol. 21, No. 6, pp290-296, (1980).

4 M. V. Swain and J. C. Metras, “Median Crack Initiation and Propagation Beneath a Disc Glass Cutter”, Glass Technology, Vol. 22, No. 5, pp222-230, (1981).

5 M. V. Swain, “The Breaking of Scored Glass”, Glass Technology, Vol. 23, No. 2, pp120-124, (1982).

6 T. Ono and K. Tanaka, “The Theoretical and Quantitative Evaluation of the Cuttability of AMLCD Glass Substrates using Four-Point-Bending Test”, Journal of the SID, Vol. 7, [3], pp207-212 (1999).

7 Weili Cheng and Iain Finnie, “A Prediction on the Strength of Glass Following the Formation of Subsurface Flaws by Scribing”, Journal of The American Ceramic Society, 75, [9], pp2565-2572, (1992).

8 S. M. Widerhorn, “Influence of Water Vapor on Crack Propagation in Soda-Lime Glass”, Journal of The American Ceramic Society, 50, [8], pp407-414, (1967).

9 STRESS INTENSITY FACTORS HANDBOOK, Vol. 1, Committee on Fracture Mechanics, The Society of Materials Science, Japan, Editor-in-chief, Y. Murakami, Pergamon Press, pp16-17, (1986).

10 K. Tanaka, “Elastic/plastic indentation hardness and indentation fracture toughness: the inclusion core model”, Journal of Material Science, 22, pp1501-1507, (1987).

11 K. Tanaka, M. Kanari, and M. Matsui, “A Continuum Dislocation model of Vickers Indentation on a Zirconia”, Journal of Material Science, 47, pp2243-2257 (1999).

12 J. D. Eshelby, “The determination of the elastic field of an ellipsoidal inclusion, and related problems”, Procedure of Royal Society, A241, pp376-396 (1957).

13 K. Tanaka, “Stress intensity factor of a penny-shaped crack crossing a misfitting spherical inclusions”, Scripta Metallurgica, 19, pp1183-1184, (1985).

14 T. Ono ” Effect of scribing wheel dimensions on the cutting of LCD glass substrate”, SID 00 Digest, 13-1, pp156-159, (2000).

15 “Process technology of LCD panel manufacturing” EXTRA series No. 21, edited by K. Kawauchi, TRICEPS, P24, (1991).

T. Ono received his B.S. and M.S. degrees in inorganic chemistry from Nagaoka University of Technology, Niigata Japan, in 1988 and 1990, respectively. In 1990, he joined the Shizuoka Technical Center of Corning Japan K. K. where he has been engaged in research and development of finishing technologies of LCD glass and memory disc substrates. He is a member of SID and Ceramics Society of Japan.

K. Tanaka is Professor of Materials science and engineering group in department of Mechanical engineering at Nagaoka University of Technology, Nagaoka, Niigata. He received B.S. degree of metallurgy from Yokohama National University, Yokohama, Kanagawa, in 1962, and a Ph.D. in Tokyo Institute of Technology in 1970. His primary research interests are Micro-Tribology, Nano-Indentation and Nano Technologies. He was awarded Henderson Prize in 1978 and Nishiyama Prize in 1984 from The Iron and Steel Institute of Japan, and Best Paper Award of Materials Strength in 1997 from The Japan Society of Mechanical Engineers. He is a member of the Iron and Steel institute of Japan, the Japan Institute of Metal, and the Japan Society of Mechanical Engineers.

North America and all other Countries
Corning Display Technologies
MP-HQ-W1
Corning, NY 14831
United States
Telephone: +1 607-974-9000
Fax: +1 607-974-7097
Internet: www.corning.com/displaytechnologies

Japan
Corning Japan K.K.
Main Office
No. 35 Kowa Building, 1st Floor
1-14-14, Akasaka
Minato-Ku, Tokyo 107-0052 Japan
Telephone: +81 3-5562-2260
Fax: +81 3-5562-2263
Internet: www.corning.co.jp

Nagoya Sales Office
Nagoya Bldg., 7 F
4-6-18, Mei-eki, Nakamura-ku
Nagoya-shi, Aichi 450-0002 Japan
Telephone: +81 52-561-0341
Fax: +81 52-561-0348

China
Corning (China) Ltd., Shanghai Representative Office
31/F, The Center
989 Chang Le Road
Shanghai 200031
P.R. China
Telephone: +86 21-5467-4666
Fax: +86 21-5407-5899

Taiwan
Corning Display Technologies Taiwan Co., Ltd.
Room #1203, 12F, No. 205
Tun Hua North Road,
Taipei 105, Taiwan
Telephone: +886 2-2716-0338
Fax: +886 2-2716-0339
Internet: www.corning.com.tw

Korea
Samsung Corning Precision Glass Co., Ltd.
20th Floor, Glass Tower Building
946-1 Daechi-Dong
Kangnam-Ku, Seoul 135-708
Korea
Telephone: +82 2-3457-9846
Fax: +82 2-3457-9888
Internet: www.samsungscp.co.kr